Taylor & Francis
Taylor & Francis Group

ORIGINAL RESEARCH

🔓 OPEN ACCESS ⬤ Check for updates

Intracavitary adoptive transfer of IL-12 mRNA-engineered tumor-specific CD8+ T cells eradicates peritoneal metastases in mouse models

Claudia Augusta Di Trani[a,b], Assunta Cirella[a,b], Leire Arrizabalaga[a,b], Ángela Bella[a,b], Myriam Fernandez-Sendin[a,b], Joan Salvador Russo-Cabrera[a,b], Celia Gomar[a,b], Irene Olivera[a,b], Elizabeth Bolaños[a,b], José González-Gomariz[a,b], Maite Álvarez[a,b,c], Iñaki Etxeberria[a,b], Belen Palencia[a,b], Álvaro Teijeira[a,b,c], Ignacio Melero[a,b,c,d,e]*, Pedro Berraondo[a,b,c]*, and Fernando Aranda 🆔[a,b]*

aProgram of Immunology and Immunotherapy, Cima Universidad de Navarra, Pamplona, Spain; bNavarra Institute for Health Research (IDISNA), Pamplona, Spain; cSpanish Center for Biomedical Research Network in Oncology (CIBERONC), Madrid, Spain; dDepartment of Immunology and Immunotherapy, Clínica Universidad de Navarra, Pamplona, Spain; eDepartment of Oncology, Clínica Universidad de Navarra, Pamplona, Spain

ABSTRACT
Previous studies have shown that local delivery of tumor antigen-specific CD8+ T lymphocytes engineered to transiently express single-chain IL-12 mRNA is highly efficacious. Peritoneal dissemination of cancer is a frequent and often fatal patient condition usually diagnosed when the tumor burden is too large and hence uncontrollable with current treatment options. In this study, we have modeled intracavitary adoptive T cell therapy with OVA-specific OT-I T cells electroporated with IL-12 mRNA to treat B16-OVA and PANC02-OVA tumor spread in the peritoneal cavity. Tumor localization in the omentum and the effects of local T-cell encounter with the tumor antigens were monitored, the gene expression profile evaluated, and the phenotypic reprogramming of several immune subsets was characterized. Intraperitoneal administration of T cells promoted homing to the omentum more effectively than intravenous administration. Transient IL-12 expression was responsible for a favorable reprogramming of the tumor immune microenvironment, longer persistence of transferred T lymphocytes *in vivo*, and the development of immunity to endogenous antigens following primary tumor eradication. The efficacy of the strategy was at least in part recapitulated with the adoptive transfer of lower affinity transgenic TCR-bearing PMEL-1 T lymphocytes to treat the aggressive intraperitoneally disseminated B16-F10 tumor. Locoregional adoptive transfer of transiently IL-12-armored T cells appears to offer promising therapeutic advantages in terms of anti-tumor efficacy to treat peritoneal carcinomatosis.

Introduction

Peritoneal carcinomatosis (PCa) or peritoneal metastasis determines poor prognosis in cancer patients.[1–3] PCa arises from the exfoliation of malignant cells from a primary tumor located within the peritoneum or from the dissemination of extraperitoneal primary tumors through the systemic route.[4] These tumor cells are shed and float in the peritoneal fluid, eventually seeding onto the peritoneal surfaces. The omentum represents one of the most favorable peritoneal locations for tumors to nest and, consequently, for the PCa to progress.[5–8] This is probably due to its fat reservoir, abundant vascularization, tissue regeneration features, and the presence of tolerogenic immune cells.[8–10] Paradoxically, in normal conditions, the omentum is considered "the policeman of the abdomen" as it is responsible for peritoneal protection against multiple pathogens (viruses, bacteria, etc.). This function is mediated by immune aggregates that are historically called "milky spots".[11–13] Taken together, the omentum's characteristics in PCa makes it an attractive target to modulate in cancer treatment.[13–15]

Peritoneal dissemination of most cancers was diagnosed as a final and often untreatable stage until recently. Over the past three decades, advances in surgery in combination with intraperitoneal chemotherapy have opened up the field of locoregional treatment of PCa.[16,17] However, these treatments have not shown acceptable efficacy in terms of improving overall survival, which explains the high rates of morbidity and mortality in this disease.[18] Hence, new locoregional immunotherapy approaches are being exploited.[19–23]

Adoptive T cell immunotherapy (ACT) is one of the most widely explored immunotherapy strategies in the treatment of solid tumors, and many gene engineering methods are being implemented to overcome the intrinsic limitations of the approach.[24] CAR T cells armored to secrete the pro-inflammatory cytokine interleukin 12 (IL-12) have been tested and have shown anti-tumor effects in solid tumors with limited side effects.[25–28] Only recently, the intraperitoneal injection of CAR T cells has been used in humans for the first time, in clinical trials evaluating CAR T cells targeting MUC16ecto+ ovarian cancers and constitutively secreting IL-12 (NCT02498912), and targeting CEA-expressing adenocarcinoma peritoneal metastases (NCT03682744).

However, very little has been reported regarding the local peritoneal immune impact and the intracavitary mechanisms have been overlooked.

We previously reported that local/intra-tumor adoptive transfer of tumor-specific T cells, which transiently express single-chain IL-12 mRNA to mitigate toxicity, achieved pronounced anti-tumor efficacy in subcutaneously implanted tumors.[29] In this study, we evaluated the effectiveness of these transiently engineered CD8^{+} T cells against peritoneal metastasis in animal models[30] , comparing intravenous to intracavitary/locoregional delivery in terms of anti-tumoral efficacy and reprogramming of the tumor microenvironment (TME). Moreover, we thoroughly analyzed the impact of IL-12-armored locoregional delivery on the immune cell phenotype in the peritoneal cavity and omentum. In general, we determined whether this strategy could be a feasible and effective option to launch for PCa patients in clinical trials.

Material And Methods

Cell lines and culture media

B16-OVA cells were provided by Dr. Lieping Chen (Yale University, New Haven, CT, USA) in November 2001. B16-F10 cells were purchased from the ATCC in June 2006. Both cell lines were maintained in complete RPMI medium: RPMI 1640 medium with GlutaMAX (Gibco, Waltham, MA, USA) supplemented with 10% FBS (Sigma-Aldrich, St. Louis, MO, USA), 100 IU/ml penicillin and 100 μg/ml streptomycin (Gibco) and 50 μM 2-mercaptoethanol (Gibco). In the case of B16-OVA cells, the medium was supplemented with 0.4 mg/ml of G418 (Sigma-Aldrich). The PANC02-OVA cell line, kindly provided by Dr. Sebastian Kobold (University of Munich, Germany), was maintained in DMEM, high glucose (Thermo Fisher, Hennigsdorf, Germany) supplemented as in the case of RPMI. All cell lines were routinely tested for mycoplasma contamination using the MycoAlert Mycoplasma Detection Kit (Lonza, Basel, Switzerland).

mRNA synthesis by in vitro transcription (IVT)

The single-chain IL-12 sequence consists of the murine IL-12p40 subunit including its own signal peptide, but with depletion of the stop codon, followed by a flexible linker of 15 amino acids $(Gly_4Ser)_3$ followed by the murine IL-12p35 subunit deprived of its signal peptide and followed by a stop codon.[31] Firefly luciferase protein sequence was obtained from the UniProt database (# P08659). The sequences were codon-optimized for *Mus musculus* and synthetized and cloned by GenScript (Nanjing, China) in a pUC57 backbone. The sequence upstream of the first codon of the open reading frame (ORF) comprised the T7 promoter (TAATACGACTCACTATAGGG) and a Kozak sequence (GCCGCCACC). The stop codon was followed by two sequential β-globin 3′UTRs cloned head to tail and a 90–120 poly(A) tail, as optimized by Holtkamp *et al.*[32] The sequence of the generated constructs was verified by direct sequencing and double restriction enzyme digestion. The plasmids were linearized with 100 U HindIII (NEB R0104S, New England Biolabs, Ipswich, MA, USA) for each 100 μg of plasmid for 3 h at 37°C.

Linearization was confirmed by running 0.3 μg of the digested product on a 1% agarose gel in TAE buffer. The linearized template was purified by double phenol:chloroform:isoamyl alcohol 25:24:1 organic extraction and precipitated overnight (ON) with absolute ethanol at −20°C. The pellet was then washed with 70% ethanol and, once the alcohol had evaporated, resuspended in nuclease-free water. 1 μg of the DNA template was subjected to IVT using the T7 mScript_Standard mRNA Production System (Cellscript, Madison, WI, USA), which post-transcriptionally added the Cap1 structure at the 5' end and further elongated the poly(A) tail with 150 adenines at the 3' end. The *in vitro* RNA was purified with phenol:chloroform:isoamyl alcohol 25:24:1 organic extraction, followed by ammonium acetate precipitation, according to the manufacturer's instructions. The purified mRNA was eluted in RNase-free water at 1 to 2 mg/ml and stored at −80°C.

Sample processing

For organ processing, animals were sacrificed with CO_2. The outer skin of the peritoneum was carefully dissected and peritoneal lavage fluid was obtained by injecting 3 ml of ice-cold PBS (for cytokine analysis) or supplemented with 2% FBS (for flow cytometry experiments) into the peritoneal cavity and was then collected with the same syringe after gentle massage. The lavage fluid was then centrifuged at 300 g for 10 min and the supernatants frozen at −80°C for further analyses. The cell pellet was washed and processed as described below. Spleens and lymph nodes (LNs) (axillary, mandibular, and inguinal) were isolated from the mice and disrupted by mechanical force through a 70 μm filter and abundantly washed with PBS. Both splenocytes and cells from the peritoneal cavity were incubated with ammonium-chloride-potassium (ACK) lysing buffer (Gibco) for 2 min to lyse erythrocytes. The ACK buffer was diluted with an excess volume of complete RPMI medium and the cells were washed and counted. Single-cell suspensions were kept at 4°C until further analysis. For flow cytometry analysis, the omenta were excised, minced and digested with 400 U/ml of collagenase D and 50 μg/ml of DNase-I (Roche Basel, Switzerland) for 30 min at 37°C. Living cells were enriched by Percoll 35% (Merck, Darmstadt, Germany) centrifugation. For bulk RNA-Seq, isolated omenta were weighed and frozen in RNAlater Stabilization Solution (Thermo Fisher) at −80°C until RNA isolation. For histological studies, the omenta were excised at the indicated time points, formalin fixed for 24 h, dehydrated and embedded in paraffin, cut into 3 μm sections and stained with hematoxylin and eosin (H&E).

Mouse lymphocyte isolation, activation and expansion

$OVA_{257-264}$-specific CD8^{+} T cells were extracted from LNs and splenocytes of OT-I and OT-I-CD45.1^{+} transgenic mice; gp100-specific CD8^{+} T cells were isolated from the LNs and splenocytes of PMEL-1 transgenic mice. After tissue disaggregation, erythrocyte lysis and extensive wash, OT-I T cells were resuspended at a concentration of 1×10^6 cells/ml in complete RPMI medium and activated with 1 ng/ml of $OVA_{257-264}$ peptide (Invivogen, San Diego, CA, USA) for 48 h in a humidified incubator with 5% CO_2 at 37°C. PMEL-1 T cells were

resuspended at a concentration of 1.5×10^6 cells/ml in complete RPMI medium supplemented with 100 ng/ml of human gp100 peptide$_{25-33}$ (GenScript), for 48 h in the incubator. Activated T cells were then washed and resuspended in 3 times the initial volume of fresh complete RPMI medium supplemented with the recombinant human (rh) IL-2 (Proleukin, Novartis) at 50 IU/ml for 48 h in incubator.

mRNA electroporation

For mRNA electroporation, stimulated and expanded T cells were washed and resuspended in phenol red-free OPTI-MEM (Gibco) at a final concentration of 100×10^6 cells/ml. Subsequently, 2×10^7 cells were mixed with 20 µg of mRNA in 2 mm cuvettes (BioRad, Hercules, CA, USA) and electroporated using the Gene pulser Mx System (BioRad) with one 10 ms pulse of 210 V. Electroporated cells were left to rest in the incubator in complete RPMI medium supplemented with 50 IU/ml of rhIL-2 (Proleukin, Novartis). The viability of T cells was checked 1 h after electroporation by trypan blue staining and the transfection efficiency was checked by flow cytometry for the electroporated protein 6–24 h after electroporation.

Anti-tumor efficacy of adoptive T cell transfer

Experiments with mice were approved by the Ethics Committee of the University of Navarra (R-080-19GN). We have complied with all relevant ethical regulations for animal testing and research. Anti-tumor efficacy experiments were performed in 6–10-week-old C57BL/6 J mice that were purchased from Harlan Laboratories (Barcelona, Spain) and bred in our facilities (CIMA, Pamplona, Spain). B16-OVA, B16-F10 and PANC02-OVA cells were thawed one week before injection. On day 0, cells were detached with pre-warmed trypsin, washed, and counted. B16-OVA and PANC02-OVA cells were resuspended at a final concentration of 5×10^5 cells in 500 µl of PBS per mouse for the intraperitoneal (IP) injection. B16-F10 cells were resuspended at a final concentration of 2.5×10^5 cells in 500 µl of PBS for IP injection or at a final concentration of 1×10^5 cells in 100 µl of PBS for subcutaneous injection (SC) in rechallenge experiment. ACT was performed on days 6 and 9, or day 9 and 12 after tumor inoculation with 2.5×10^6 alive electroporated T cells per mouse in 500 µl PBS for IP injection and 100 µl PBS for intravenous injection (IV). Control mice were injected with the same volume of PBS. When indicated, 100 µg of αCD137 mAb (3H3 clone), αPD-1 (RMP1-14 clone) or the matched RatIgG2a isotype (BioXcell, West Lebanon, NH, USA) were injected IP on D6, 9, 12 and 15. Mice were closely observed 3 times a week and sacrificed when they gained >20% of their initial weight or when they showed other signs of distress (*e.g.* lethargy, poor mobility, poor feeding, piloerection, poor ambulation) following the Ethics Committee for Animal Experimentation guidelines.

Flow cytometry

For flow cytometry staining, cells obtained from the peritoneal lavage, the omentum and splenocytes were stained using the Zombie NIR Fixable viability kit (BioLegend, San Diego, CA, USA) or with PKPF (# 840301, PromoCell, Heidelberg, Germany) for 5 min at room temperature (RT). After being washed with staining buffer (PBS +2% FBS, 2 mM EDTA, 1% 100 IU/mL penicillin and 100 µg/ml streptomycin (Gibco)), cells were treated with FcR-Block (anti-CD16/32 clone 93; BioLegend # 101302) and then surface stained with the following fluorochrome-labeled antibodies purchased from BioLegend (unless otherwise specified) for 20 min at 4°C protected from light: PE-CY7-F4/80 # 123114, BV650-CD19 # 115541, Pacific Blue-CD45.2 # 109820, PERCP 5.5-CD45.1 # 110728, BV605-TCRb # 109241, FITC-CD4HT # 116004, BV510-CD8a # 100751, PE-CY7-CD3 # 100220, BUV395-CD8 # 563786 BD Biosciences (San José, CA, USA) BUV496-CD4 # 564667 BD Biosciences, BV605-CD90.2 # 105343, BV785-PD-1 # 135225,HT PE-Dazzle594- NK1.1 # 108747, APC-CD25 # 102012, PerCP5.5-CD45.2 # 109828, APC/Fire750-Tim-3 # 134018, PE-CD45.1 #110743, FITC-Ly6C # 128006, APC-PD-L1 # 124311, APC-eFluor780-MHCII (I-A/I-E) # 47–5321-82 eBioscience (San Diego, CA, USA), PE-Dazzle594-CD38 # 102729, BV421-F4/80 # 123131, BV510-LY6G # 127633, CD11c-BV605 # 117333, BV785-TCRb # 109249, BUV395-CD11b # 563553 BD Biosciences, PerCPeFluor710-CD3 # 46–0032-80 eBioscience, PE-Cy7-CD45 # 103114, PE-CD90.1 # 202523, BV785-CD45.1 # 110743, PE-CY7-CD45.2 # 109830.

When necessary, the Foxp3/TF staining buffer kit (eBioscience) was used according to the manufacturer's instructions for intracellular staining with AF488-Ki-67 (# 558616 BD Biosciences). After extensive washing, cells were resuspended in 150–200 µl of staining buffer and immediately assayed using a CytoFLEX flow cytometer (Beckman Coulter, Brea, CA, USA). Flow cytometry analyses were performed with FlowJo_V10 software.

RNA isolation, RNA sequencing (RNA-Seq), and data analysis

The omenta were disaggregated by mechanical homogenization while kept on ice and total RNA extraction was performed using the RNeasy Mini Kit (Qiagen, Hilden, Germany), according to the manufacturer's instructions. RNA was subjected to quantity and quality control using the Qubit HS RNA Assay Kit (Thermo Fisher Scientific, Waltham, MA, USA) and the 4200 Tapestation with High Sensitivity RNA ScreenTape (Agilent Technologies, Santa Clara, CA, USA). Library preparation was performed using the NEBNext Ultra II Directional RNA Library Prep Kit (NEB) according to the manufacturer's protocol. All sequencing libraries were constructed from 100 ng of total RNA according to the manufacturer's instructions. Briefly, the protocol selects and purifies poly(A) containing RNA molecules using magnetic beads coated with poly(T) oligos. Poly(A)-RNAs are fragmented and reverse-transcribed into the first cDNA strand using random primers. The second cDNA strand is synthesized in the presence of dUTP to ensure the specificity of the strand. The resulting cDNA fragments are purified with NEBNext purification beads, adenylated at the 3′ ends and then ligated with uniquely indexed sequencing adapters. The ligated fragments

are purified and PCR amplified to obtain the final libraries. The quality and quantity of the libraries were verified using the Qubit dsDNA HS Assay Kit (Thermo Fisher Scientific) and 4200 Tapestation with High Sensitivity D1000 ScreenTape (Agilent Technologies). The libraries were then sequenced using a NextSeq2000 sequencer (Illumina). 30–40 million pair-end reads (100 bp; Rd1:51; Rd2:51) were sequenced for each sample and demultiplexed using Cutadapt. RNA-Seq was carried out at the Genomics Unit, CIMA Universidad de Navarra (Pamplona, Spain).

For the analysis of the RNA-Seq data, first, quality control of all samples was performed with the FastQC tool (http://www.bioinformatics.bbsrc.ac.uk/projects/fastqc). Before alignment, low quality reads and adapters were removed with Trimmomatic[33] A raw count matrix was obtained using the STAR aligner[34] with a mm39 assembly and annotated with Gencode version M27. The analysis of differentially expressed genes was carried out in R/Bioconductor following the workflow provided by limma-voom[35] using linear models. First, genes with less than five counts in all samples (non-expressed genes) were removed from the analysis prior to normalization. The data sets were normalized using TMM (trimmed mean of M-values), then the $\log_2$ counts per million reads (CPM) values were calculated and the expression matrix was used for the statistical analysis. We selected the set of differentially expressed genes for each comparison (adj. p-value < 0.05 and logFC <-1 | >1). Gene ontology enrichment analysis was performed with the differentially expressed genes of the OT-I-IL-12-IP treatment *vs.* OT-I-IL-12-IV with the clusterProfiler package[36] using the biological process ontology as reference. RNA-Seq reads were deposited in the Gene Expression Omnibus (GEO) database of the National Center for Biotechnology Information and are accessible through GEO Series accession number GSE197612.

Luminescence detection with PhotonIMAGER

Six days after B16-OVA IP tumor inoculation (or PBS injection in mice with no tumor), 2.5×10^6 OT-I cells electroporated with a luciferase-coding mRNA were injected either intraperitoneally or retro-orbitally. 5 h after injection, *in vivo* and *ex vivo* bioluminescence was detected to visualize OT-I T cells localization following the different route of administration. To this end, 100 μl of luciferin (Promega, Madison, WI, USA) (20 mg/ml) was administered IP. After 5 min, the spleen, omentum, and mesentery of each mouse were collected and bioluminescence was detected using PhotonIMAGER TM (Biospace Lab, Paris, France). Data were analyzed using M3 Vision software.

Cytokine analyses

IFN-γ and IL-12 protein levels in the serum and peritoneal lavage fluid from the mice were assayed by enzyme-linked immunosorbent assay (ELISA) (BD Biosciences # 555138 and # 555256), following the manufacturer's instructions. Data were analyzed and interpolated into the standard curve values using GraphPad Prism V.8.2.1 software (GraphPad Software, San Diego, CA, USA).

A total of 8 cytokines were simultaneously measured in serum and peritoneal lavage samples of mice bearing or not B16-OVA IP tumors or in peritoneal lavage fluids of mice bearing B16-F10 IP tumors, 18 h after injection of OT-I adoptive T cell transfer and 19 h after injection of PMEL-1 ACT using the ProcartaPlex Multiplex Immunoassay (Thermo Fisher Scientific), following the manufacturer's instructions. The data were acquired using the Luminex MAGPIX instrument system (Thermo Fisher Scientific).

For ELISpot experiments (BD Biosciences), splenocytes were isolated and erythrocytes lysed as described above. Briefly, 0.4×10^6 splenocytes were either stimulated with 0.001 mg/ml OVA$_{257-264}$ peptide or incubated with complete medium only (for unstimulated controls) for 21 h in anti–IFN-γ capture antibody-coated plates. After extensive washing, plates were incubated with the biotinylated detection antibody for 2 h at RT. The wells were washed and incubated with the Streptavidin-HRP solution for 1 h at RT. 1X AEC Substrate Solution was added to the wells for 1–2 min, and then these were rapidly soaked in DI water to stop the reaction. Plates were left drying ON and spot-forming cells were automatically counted using an ImmunoSpot counter (CTL-Immunospot; Bonn, Germany).

Statistical analysis

GraphPad Prism was used for statistical analysis. Data were analyzed by two-tailed unpaired t-test or two-way or one-way analysis of variance followed by Sidak's or Tukey's multiple comparison test. Survival analysis was performed using the Kaplan–Meier method. The Log-rank test was used to statistically compare the curves. Values of p < 0.05 were considered statistically significant.

Results

Intraperitoneal adoptive T cell transfer results in a more robust pro-inflammatory tumor microenvironment than the intravenous route

The omentum is a common site of metastases arising from intraperitoneal tumors. To model this disease scenario in murine models, we injected the B16 cell line expressing ovalbumin (B16-OVA) IP in mice.[10,37] Six days after tumor inoculation, dark tumor foci were macroscopically detectable in the omentum of mice (Figure 1a) and hematoxylin and eosin staining showed how, at this time point, tumor cells had infiltrated and colonized the omentum, displacing adipocytes almost completely, compared to control mice injected with saline solution alone (**Fig. S1A**). Therefore, day 6 was selected as the first time point to evaluate the efficacy of adoptive transfer of mRNA-electroporated tumor-specific T lymphocytes (Figure 1b). In order to study the biodistribution of T cells after adoptive transfer, we electroporated OT-I T cells, which express an OVA$_{257-264}$-specific TCR, with a luciferase (LUC)-coding mRNA. As summarized in Figure 1c, 2.5×10^6 cells were injected IP or IV. 5 h after T cell injection, we analyzed the *in vivo* and *ex vivo* bioluminescence catalyzed by the *in vivo* translated protein and interpreted the emission point as the
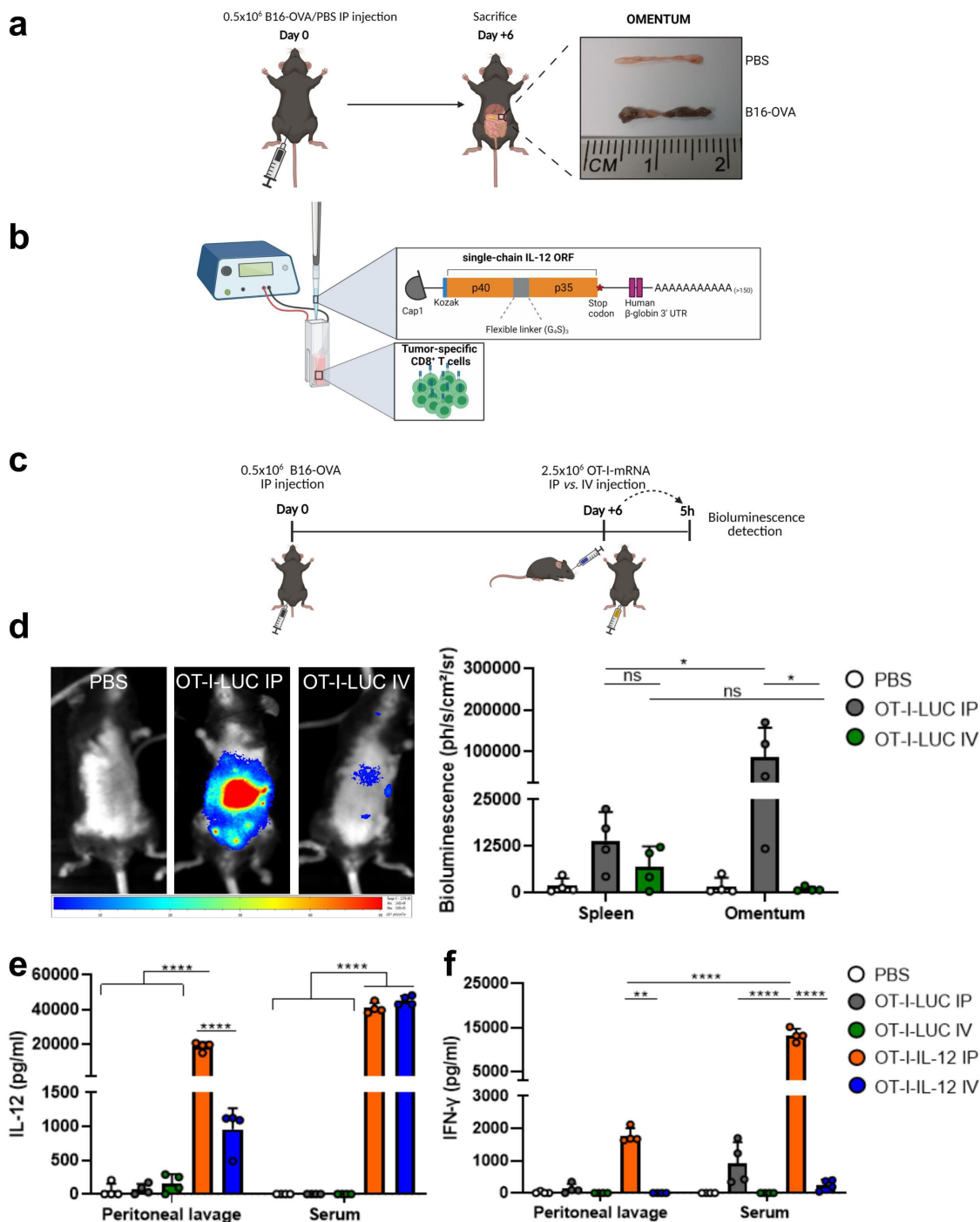
Figure 1. Intraperitoneal transferred T cells home to the omentum, leading to the higher expression of the electroporated IL-12 payload in the peritoneum compared to systemic delivery. a. Representative omentum, isolated from a mouse six days after B16-OVA or PBS IP injection, showing the localization of tumor cells in the organ at this time point. **b**. Schematic representation of the *in vitro* synthetized IL-12 mRNA, which is mixed with the tumor-specific T cells just prior to their electroporation. **c**. The scheme summarizes the experimental setting employed in panels d-f: C57BL/6 J mice were injected intraperitoneally with 0.5×10^6 B16-OVA cells. Six days later, mice were injected with LUC- or IL-12 mRNA-electroporated OT-I T cells either intraperitoneally or retro-orbitally (*n* = 4/group). **d**. 5 h after ACT, *in vivo* bioluminescence (on the left) and *ex vivo* bioluminescence (on the right) of spleen and omentum were detected. **e, f**. The production of IL-12 and IFN-γ was measured by ELISA 5 h after adoptive cell transfer. Data are given as mean ± SD in panels. **d, e and f**. Statistical significance was determined with two-way Anova with Sidak's multiple comparison test for Figure 1d, and with Tukey's multiple comparison test for **e** and **f**. (*p < 0.05, **p < 0.01, ****p < 0.0001).

site of T-cell localization at the chosen time point. IP injected T cells accumulated primarily in the omentum, with detectable signal also in the spleen. In contrast, IV injection promoted T-cell homing to the spleen, but not to the omentum (Figure 1d). The appearance of T cells in the omentum after

IP transfer was independent of the presence of the tumor in the peritoneal cavity (**Fig. S1 B, C**).

Next, we evaluated the concentration of IL-12 and IFN-γ in peritoneal lavage fluids and in sera 5 h after IP or IV transfer of OT-I T cells electroporated with mRNA encoding either

murine single-chain IL-12 or luciferase, as an irrelevant control mRNA. High levels of IL-12 were detected in the peritoneal lavage fluid of mice IP injected, while significantly lower levels were observed in those injected via the IV route. In serum, comparable concentrations of IL-12 were found using both delivery methods (Figure 1e). In contrast, IFN-γ, the most relevant downstream effector of IL-12, was detected at significant levels only in the peritoneal lavage fluids and in the sera of mice treated locoregionally (Figure 1f).

To evaluate whether higher production of IL-12, IFN-γ or other pro-inflammatory cytokines depended on the rapid recognition of tumor antigens by locoregionally injected T cells, we performed a multiplex cytokine assay in the peritoneal lavage fluid and serum samples from mice bearing or not B16-OVA tumors, 18 h after IV or IP injection of OT-I-IL-12. In the peritoneal lavage samples, a marked increase in all the cytokines analyzed in tumor-bearing mice was detected when treated intraperitoneally as compared to IP treated tumor-free mice and IV injected tumor-bearing mice. In addition to IL-12 and IFN-γ, other induced cytokines included pro-inflammatory cytokines such as IL-6, IL-2 and TNF-α, and cytokines promoting or attracting macrophages such as M-CSF, GM-CSF and CCL3 (Figure 2a). In serum, IL-12 concentration levels were comparable in tumor-bearing and tumor-free mice, whereas IFN-γ was only detected in tumor-bearing mice when treated intraperitoneally. In 2 out of 4 mice, measurable levels of IL-6, IL-2 and TNF-α were observed in the sera of IP treated tumor-bearing mice (**Fig. S2A**).

Taken together, our results show that intraperitoneally injected T cells rapidly home to the omentum and that their immediate co-localization with tumor antigens contributes to the increase in the production of several pro-inflammatory cytokines.

The locoregional adoptive transfer of T cells that transiently express IL-12 results in better overall survival compared to the systemic delivery route

To investigate whether the benefits of the locoregional treatment resulted in a higher anti-tumor response, we treated B16-OVA-bearing tumor mice with two doses of OT-I T cells electroporated either with IL-12- or LUC-coding mRNAs. Irrelevant mRNA-electroporated T cells did not have any effect on mice survival, while OT-I-IL-12 treatment induced a significant increase in survival when compared to control mice. The best results were obtained by IP injection, which resulted in almost 100% mice survival. Thus, IP delivery proved to be much more effective than intravenous administration in this setting (Figure 2b). Indeed, locoregional delivery of IL-12 mRNA-armored T cells rescued 100% of mice from peritoneal carcinomatosis even when therapy was started at later time points (on days 9 and 12) (**Fig. S2B**).

To better understand how the different routes can reprogram the TME, we performed a bulk RNA-Seq of omenta excised from mice 18 h after treatment with IP OT-I-IL-12, IV OT-I-IL-12 or PBS injection. As observed in the volcano plots, IP treatment led to the up-regulation of 1867 genes and to the down-regulation of 1526 genes with respect to the PBS group (Figure 3a). IV treatment also induced significant

changes, but these were lower when compared to the IP route (902^{up} vs. 146_{down}) (Figure 3b). 855 genes were commonly modulated by the two administration routes, while 2538 were specific to the IP route (Figure 3c and **Fig. S3A, B**). Interestingly, within the set of genes that were similarly modulated, those related to a T helper 1 (Th1)-polarized TME, such as IFN-γ, granzyme B and IFN-γ-induced transcripts such as PD-L1 and IDO1 and chemokines such as CXCL10 and CXCL11 were among the genes up-regulated and significantly more up-regulated in the IP-treated group vs. the IV-treated group. The gene ontology enrichment analysis identified several immune-related terms up-regulated by the intraperitoneal administration with respect to the intravenous route. Among the down-regulated terms, several involved in fatty acid metabolism were identified, indicating some level of metabolic reprogramming of cells in the omentum (Figure 3d-e and **Fig. S3**).

The top up-regulated terms were those related to leukocyte migration and positive regulation of cytokine production (Figure 3d, f, g, and **Fig. S3B**).

Collectively, these results suggest that the intracavitary administration route triggers a favorable early transcriptional reprogramming of the TME and an enhanced anti-tumor efficacy as compared to the systemic route.

IL-12-armoring of transferred T cells modulates the phenotype of various subsets of immune cells in the peritoneal cavity and the omentum

Given the unambiguous evidence of the superiority of the locoregional delivery, we next decided to further characterize the mechanisms underlying the potent effect achieved by this delivery route.

The paracrine effects of the released IL-12 on the anti-tumor response triggered by tumor-specific T cells were further investigated by analyzing the phenotype of the IL-12-sensing immune subsets, including T cells and NK cells, and of the IFN-γ-sensing myeloid compartment.

To this end, 21 h after injection of PBS or OT-I T cells (derived from CD45.1[+] syngeneic mice to allow their discrimination from endogenous T lymphocytes), cells were recovered from peritoneal lavage fluids (**Fig. S4A**) and excised omenta (**Fig. S4B**) and stained for flow cytometry analyses. In both compartments, IL-12 engineering of tumor-specific T cells induced significantly enhanced expression of the high-affinity receptor of IL-2 (CD25) (as already demonstrated[38]) with respect to LUC-electroporated T cells, thus contributing to more pronounced proliferation of OT-I T cells and clonal expansion in this treatment condition. Such significant up-regulation was also observed among endogenous CD45.2^{+} CD8^{+} T cells in mice treated with IL-12-armored adoptive T cell transfer. Exogenous T cells (electroporated with LUC or IL-12 mRNA) were highly proliferative (almost 100% were Ki-67^{+}) and expressed similar levels of PD-1 and PD-1/Tim-3.

As shown in **Fig. S5A-B**, IL-12-armoring of T cells promoted a significant increase in CD25 expression in NK cells both in the peritoneal cavity and in the omentum and of the activation markers CD90.2[39] and PD-1 in the peritoneal cavity.
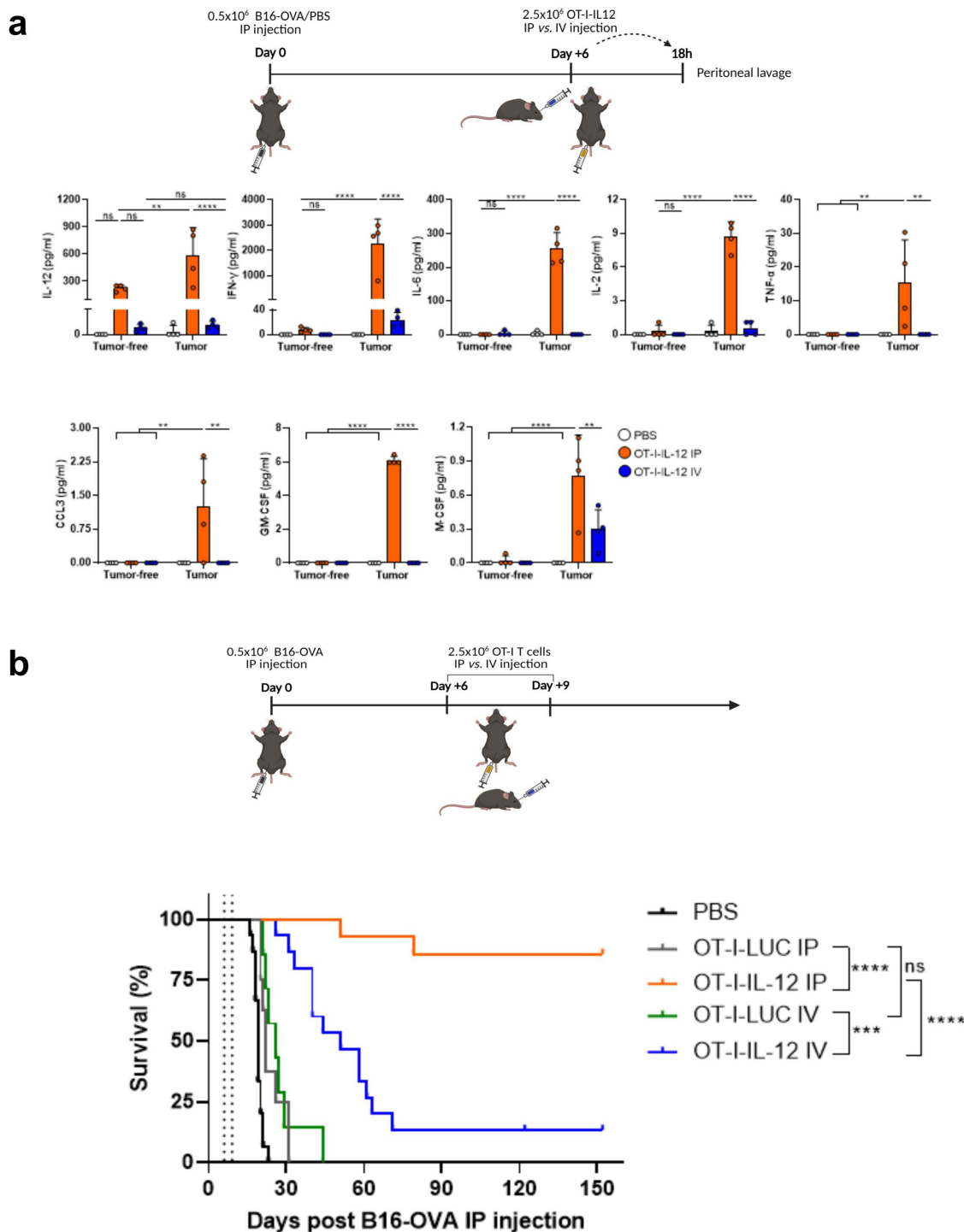
Figure 2. Locoregional injection of OT-I-IL-12 cells results in a pro-inflammatory TME and a potent anti-tumor effect. a. A schematic representation of the dose regimen followed is shown. 18 h after adoptive cell transfer, the concentration of 8 cytokines was measured in the peritoneal lavage fluid of mice by a ProcartaPlex multiplex immunoassay ($n = 4$/group). **b**. Survival follow-up of mice treated with OT-I-LUC or OT-I-IL-12 intraperitoneally or systemically (pool of two independent experiments). Treatment days are indicated by the dashed lines. (PBS group $n = 15$; OT-I-LUC IP and OT-I-LUC IV $n = 7$; OT-I-IL-12 IP $n = 14$; OT-I-IL-12 IV $n = 15$). Data are given as mean ± SD. Statistical significance was determined with two-way Anova with Tukey's multiple comparison test for panel **a**. Survival differences between groups, in panel **b**, were analyzed using Log-rank tests (Mantel-Cox). (**$p < 0.01$, ***$p < 0.001$, ****$p < 0.0001$).

IL-12, and its downstream signaling, reportedly exerts its potent anti-tumor effect also by acting on the myeloid compartment.[40,41] In the peritoneal cavity, myeloid leukocytes from mice treated with adoptive transfer compared to those injected with PBS appeared markedly different based on forward and side scatter profiles in flow cytometric analyses (**Fig. S5C**, left panel, which shows the backgating of large

peritoneal macrophage population (LPM), which is described further in the text). Indeed, as represented in the right panel of **Fig. S5C**, intraperitoneal transferred tumor-specific T cells (electroporated with LUC or IL-12) induced an almost total ablation of the LPMs at this time point. LPM constitute an embryonically seeded and long-lived macrophage population that normally accounts for the majority of the macrophage
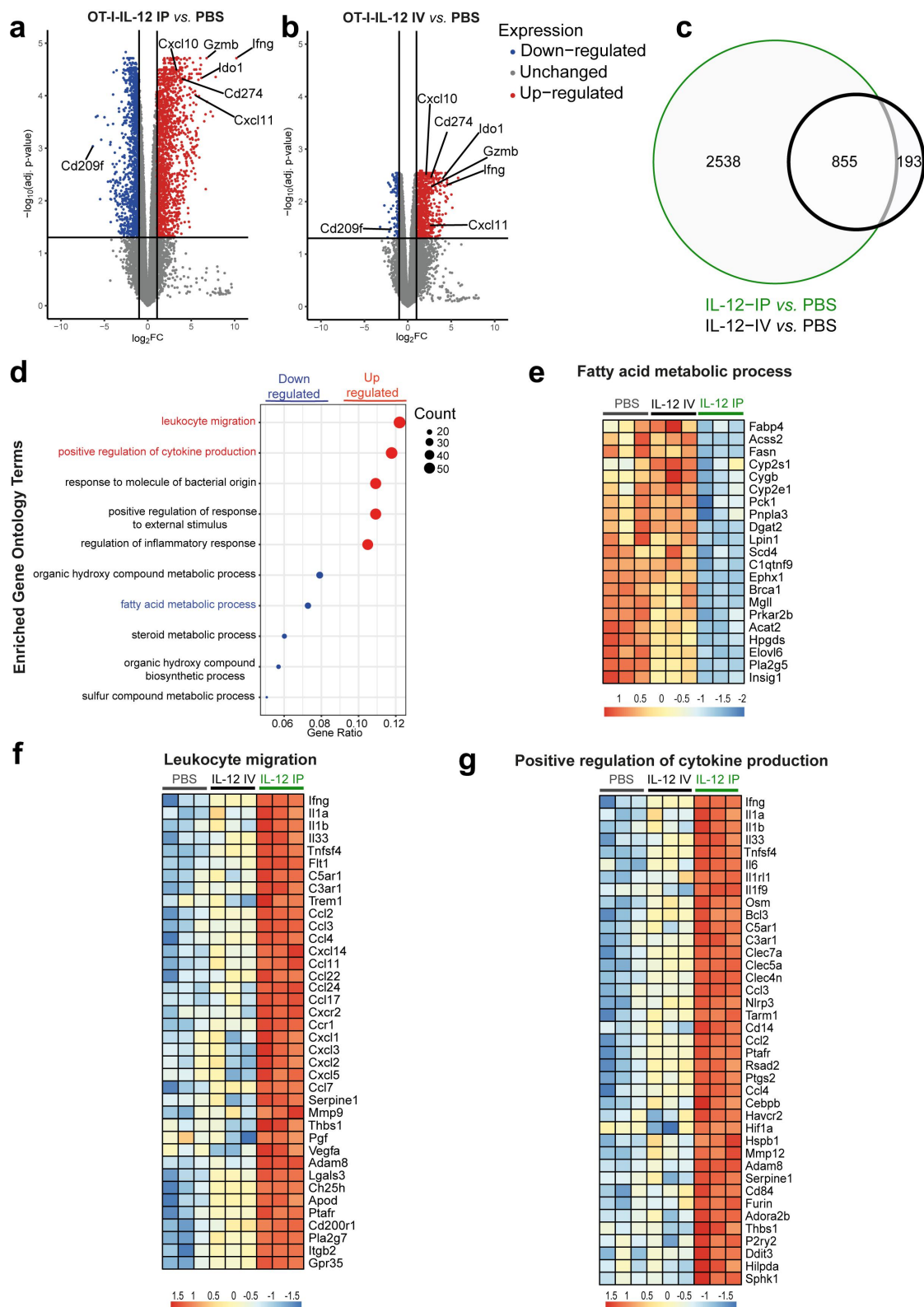
Figure 3. Bulk RNA-Seq of the omentum of mice treated with OT-I-IL-12 shows an early favorable modulation of chemokines and cytokines and reduced fatty acid metabolism when treated locoregionally. a, b. C57BL/6 J mice were treated with OT-I-IL-12 T cells 6 days after challenge with B16-OVA cell line. 18 h after ACT, the omenta were processed and bulk RNA-Seq (n = 3/group) was performed. Volcano plots showing the differentially expressed genes (adj. p-value<0.05; logFC< −1| >1) within each treatment with respect to the PBS group. The dots indicate the most relevant modulated genes. **c.** Venn diagram indicating the number of differentially expressed genes (adj. p-value < 0.05; logFC < −1 | >1) between each treatment *versus* the PBS group. The overlap indicates the number of genes that both treatments significantly modulate with respect to the PBS condition. **d**. The panel reports the five most up-regulated (red dots) and the five most down-regulated (blue dots) terms after gene ontology enrichment analysis of the differentially expressed genes between the OT-I-IL-12 IP-treated group *vs*. the OT-I-IL-12 IV-treated group. **e, f, g** Heat maps showing the Z-scored $\log_2$ (CPM) expression of enriched genes between the two routes of treatment in the following gene ontology terms: fatty acid metabolism, leukocyte migration, and cytokine production (adj. p-value < 0.05; logFC < −1 | >1).

compartment in the peritoneal cavity and whose targeted depletion has been shown to improve PCa prognosis.[5,42,43]

Regarding small peritoneal macrophages (SPM), which differentiate from bone marrow-derived Ly6C^{hi} classical monocytes, the degree of replacement appears to correlate with the extent of induced loss of LPMs.[44] In fact, in **Fig. S5D**, we observed a higher number of inflammatory Ly6C^{hi} monocytes after treatment that were also characterized by up-regulation of CD38, whose expression is known to be up-regulated by IFN-γ.[45,46] Up-regulation of CD38 is reportedly required for trans-migration through endothelial cells,[47] more efficient phagocytosis[48] and antigen presentation.[49] Of note, we observed a significant up-regulation of PD-L1 in these monocytes following OT-I adoptive transfer, most likely due to locally high levels of IFN-γ.

Collectively, our data show that intraperitoneal delivery of IL-12-engineered tumor-specific T cells promotes the proliferation and activation of exogenous and endogenous CD8^{+} T cells, of NK cells and leads to the contraction of the peritoneum-resident macrophage population.

IL-12-engineered transferred T cells are conferred with longer persistence to exert a more durable anti-tumor immunity

To assess how IL-12 mRNA-armoring affected the persistence of transferred T cells *in vivo*, we evaluated the presence of transferred CD45.1[+] OT-I T cells in mouse blood over time (Figure 4a). More than one month after adoptive cell transfer, 100% of IL-12-treated mice showed detectable exogenous T cells in peripheral blood, and 77 days after the inoculum 75% of mice still did so.

Apart from peripheral blood, OT-I-IL-12 treated mice showed a significantly higher percentage of transferred T cells in their omenta, peritoneal lavage fluids, and spleens compared to OT-I-LUC treated mice six days after the second cellular dose (Figure 4b-d). Furthermore, at this time point, splenocytes were tested for IFN-γ production upon *ex vivo* antigen stimulation using the ELISpot assay. Splenocytes from mice treated with OT-I-IL-12 exhibited the highest number of IFN-γ-producing T cells, which were significantly higher when compared to the response observed in the OT-I-LUC and PBS groups, most likely due to the accumulation of higher numbers of functional tumor-specific T lymphocytes (Figure 4e, **Fig. S4**). Taken together, these results demonstrate that the transient expression of IL-12 significantly increases the persistence of the transferred T cells, thus overcoming an important hurdle for adoptive T cell transfer applicability. Next, we evaluated the generation of immune memory in mice that fully eradicated the peritoneal tumor after OT-I-IL-12 IP treatment (Figure 4f, upper panel). 54 days after the second treatment, these tumor-free mice were re-inoculated with 1×10^5 B16-F10 cells SC in the right dorsal flank. 87.5% of mice that had overcome the primary tumor did not engraft the secondary non-OVA expressing SC tumor inoculum, whereas 87.5% of *naïve* mice used as controls did (Figure 4f, lower panel). Figure 4g shows a representative tumor 7 days after tumor inoculation in *naïve* mice. In contrast, in most of the previously treated mice, tumors were not detected and, in some cases, necrotic tissue was observed. Thus, IP OT-I-IL-12 treatments triggers the generation of immune memory toward endogenous antigens of the B16 melanoma cell line.

Locoregional IL-12-armored adoptive transfer is highly efficient in other PCa tumor models

Peritoneal carcinomatosis of pancreatic origin implies a poor prognosis in humans.[50] Therefore, we challenged our adoptive immunotherapy to treat mice suffering from disseminated PANC02-OVA tumors in the peritoneal cavity. In this model, tumor-specific IL-12-engineered T cells were able to exert durable anti-tumor immunity (Figure 5a), whilst LUC-electroporated OT-I T cells were unable to control peritoneal carcinomatosis.

Since OVA-specific OT-I T cells carry a high-affinity TCR, we sought to study if PMEL-1 T cells, which bear an intermediate affinity TCR specific for the melanocytic protein gp100,[51,52] could also be strengthened in their anti-tumor performance by electroporation of IL-12 mRNA.

Therefore, we inoculated mice with 2.5×10^5 B16-F10 cells IP and treated them with two doses of PMEL-1-LUC or PMEL-1-IL-12. In this setting, IL-12 electroporation was still able to achieve a better anti-tumor response with a significant increase in survival when compared to control groups, although to a lesser extent compared to the adoptive transfer of high affinity TCR (Figure 5b). We sought to investigate the reasons for such a lower efficacy. Using ELISA assays on the supernatant of OT-I/PMEL-1 T lymphocytes left *in vitro* for 6 h after electroporation, we did not observe significant differences in their ability to secrete IL-12 or IFN-γ in culture (**Fig. S6A**). Furthermore, incubation with the cognate antigenic peptide increased production of IL-12 in both models to a similar degree (**Fig. S6A**). Furthermore, *in vivo* cytokine analysis, using the same multiplex cytokine assay as in OT-I ACT, reflected lower levels of IL-12 and of the induced cytokines in the peritoneal lavage fluid and serum 19 h after administration of electroporated PMEL-1 T lymphocytes (Figure 5c and **Fig. S6B**), compared to electroporated OT-I cells (Figure 2a and **Fig. S2A**).

To see how the lower expression of the immunostimulatory cytokine affected the phenotype of different leucocyte populations, we stained cells obtained from omenta and peritoneal lavage fluids 19 h after immunotherapy injection for further flow cytometry analyses.

At the studied time point, we observed a similar IL-12-dependent phenotype of transferred PMEL-1 T cells compared to OT-I T cells in both compartments (**Fig. S7A, B**). Interestingly, a weaker expression of CD25 was observed in endogenous CD8^{+} T cells in the peritoneal cavity of PMEL-1-IL-12 compared with OT-I-IL-12 (11% *vs.* 46%) and no up-regulation of this surface marker was found in this population in the omentum, unlike what was observed in the OT-I model (**Fig. S4A, B**).

Transient engineering of PMEL-1 T cells with IL-12 induced a brighter expression of CD25 in NK cells in the peritoneal cavity and omentum and of PD-1 in the peritoneum, but not of CD90.2, in contrast to what was observed in the OT-I model (**Figs. S8A, B; S5A, B**).
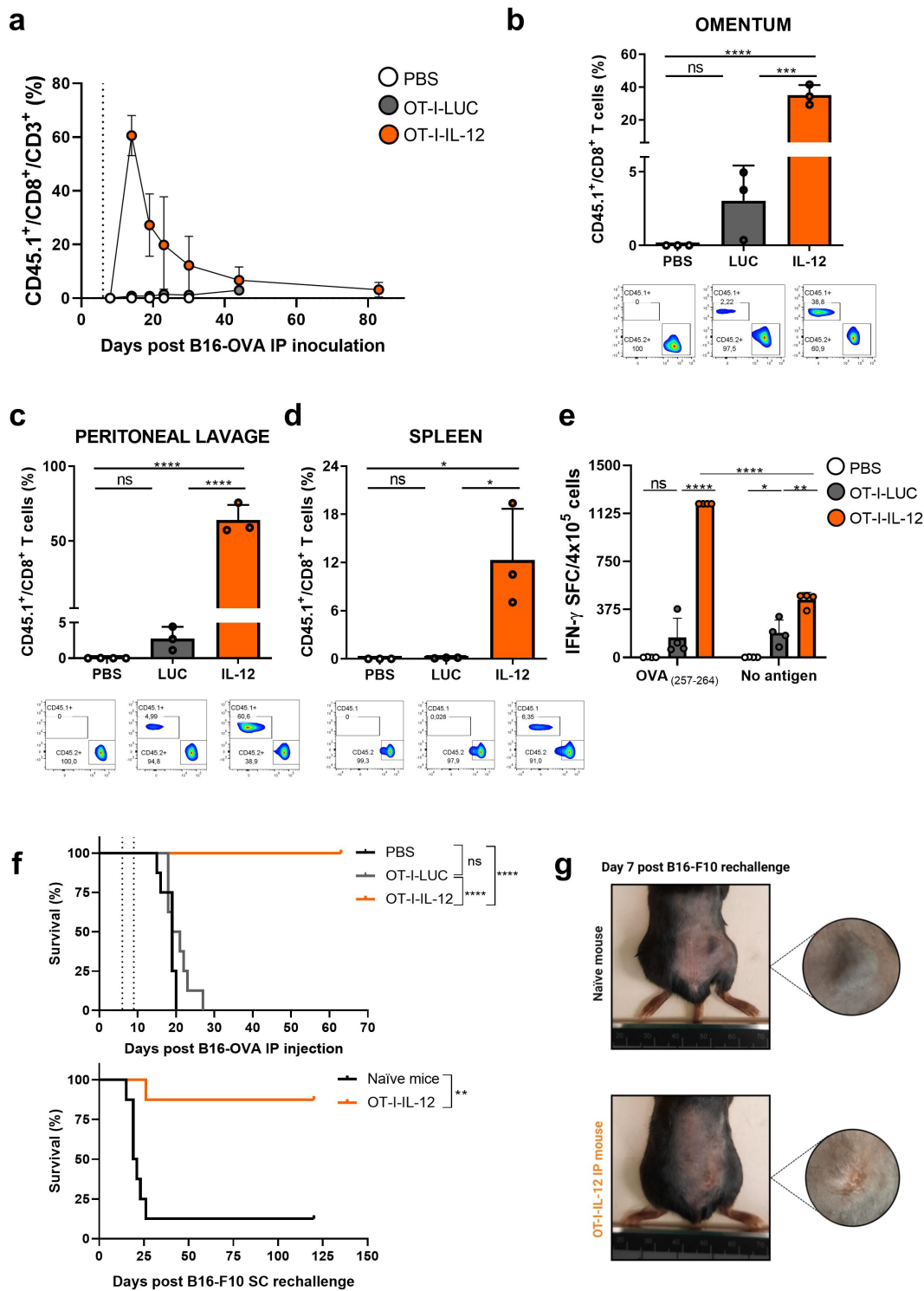
Figure 4. Electroporated IL-12 mRNA induces a higher persistence of the transferred tumor-specific T cells and protects mice from tumor rechallenge. a. Expansion of CD45.1$^+$ OT-I T cells was assessed by peripheral blood flow cytometry at the indicated time points after a one dose injection on day 6 after tumor inoculation. The injected CD45.1$^+$ OT-I T cells were gated as: viable CD19$^-$ F4/80$^-$ TCRβ$^+$ CD8$^+$ CD45.1$^+$ cells. **b-e** Organs were isolated on day 15, after a two-dose regimen with 2.5 × 10^6 T cells on day 6 and day 9. **b-d**. Omenta, peritoneal lavage fluids and spleens were isolated from control mice and mice IP treated with OT-I-LUC or OT-I-IL-12 (n = 3/group). The dot plots are representative of one mouse per group. **e**. 0.4 × 10^6 splenocytes were stimulated with 0.001 mg/ml OVA$_{257-264}$ peptide or with medium alone and incubated on an IFN-γ ELISpot plate. After 21 h, the spot-forming units were counted with an automated ImmunoSpot counter. **f**. Previously B16-OVA-cured mice (n = 8), following the adoptive transfer of IP OT-I-IL-12 (survival shown in the upper panel), were rechallenged with SC injection of the parental cell line B16-F10 on day 63, and survival was monitored as shown in the bottom panel. **g**. The picture of a representative mouse/group is shown, 7 days after the SC B16-F10 inoculum.
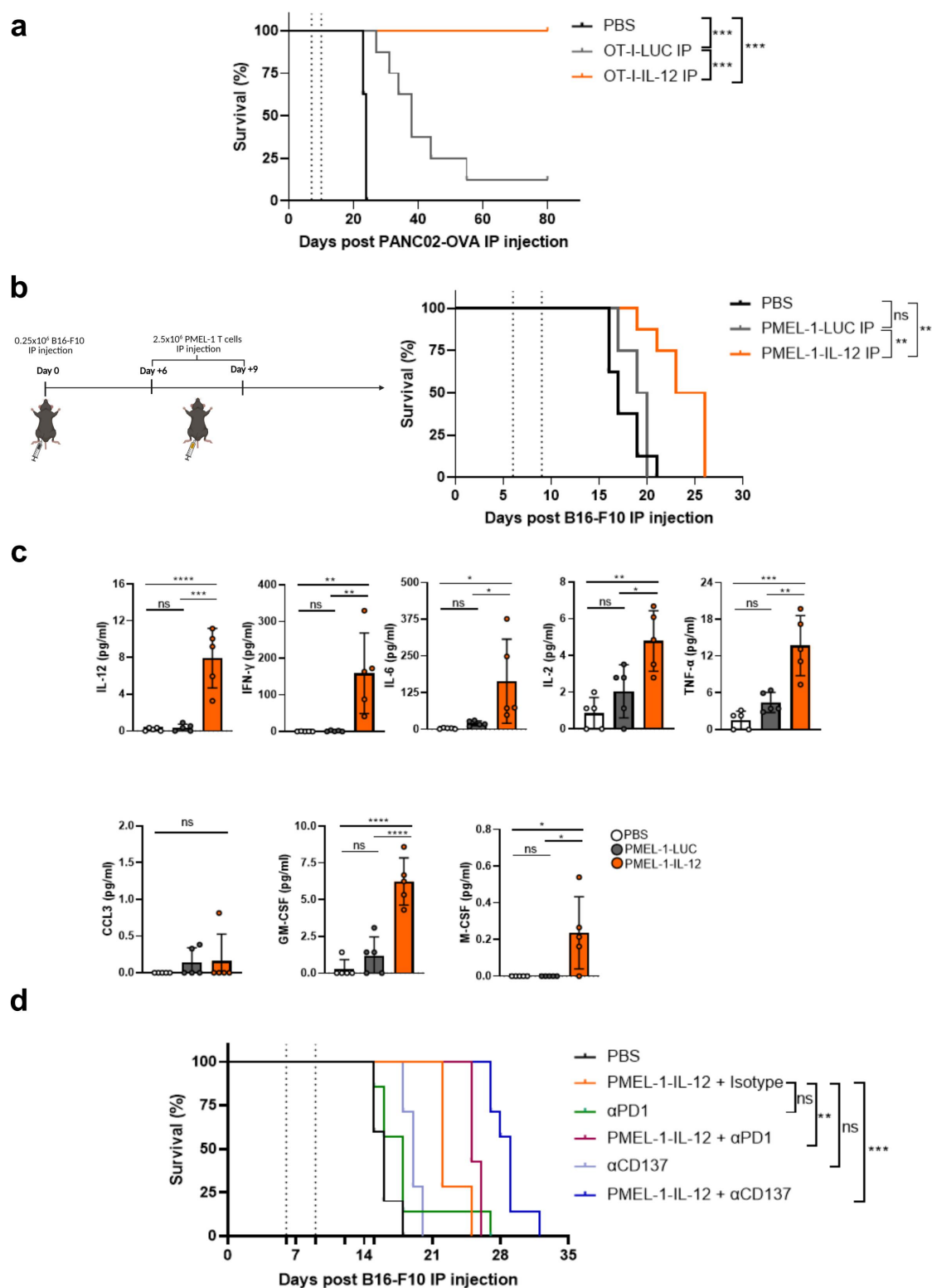
Figure 5. IL-12 mRNA-armoring of T cells enhances the anti-tumor effect of OT-I in other tumor models and of the low affinity TCR tumor-specific T cells. a. Survival follow-up of mice (*n* = 8/group) that were IP injected with PBS, OT-I-LUC or OT-I-IL-12 in IP-bearing PANC02-OVA mice is shown. Treatment days are indicated by the dashed lines. **b-d**. Mice were inoculated with 2.5×10^5 B16-F10 intraperitoneally **b**. Mice were treated with 2.5×10^6 PMEL-1 T cells on days 6 and 9, and their survival was monitored (*n* = 8). **c**. 19 h after IP injection of PBS, PMEL-1-LUC or PMEL-1-IL-12, the concentration of 8 cytokines was measured in the peritoneal lavage fluid using a ProcartaPlex multiplex immunoassay (*n* = 5/group). **d**. Mice were IP injected either with saline solution or with two doses of OT-I-IL-12. Adoptive transfer therapy was combined either with a Rat IgG2a isotype control or with antibody against PD-1 (RMP1-14 clone) or CD137 (3H3 clone) on days 6-9-12-15. Data are given as mean ± SD. Statistical significance was determined with one-way Anova with Tukey's multiple comparison test for panel C. Survival differences between groups in panels **a**, **b**, and **d** were analyzed using log-rank tests (Mantel-Cox). (*p < 0.05, **p < 0.01, ***p < 0.001, ****p < 0.0001).

In **Fig. S8C**, we show how the adoptive transfer resulted in a significant contraction of the LPMs, with respect to the PBS-injected group, and an almost complete depletion when the injected cells were engineered with IL-12 mRNA. In the OT-I case, mock electroporated T cells were sufficient to induce such a depletion, whereas IL-12 was necessary, in the PMEL setting, to cause depletion of LPM. LPM contraction was accompanied by a compensatory increase of Ly6C^{hi} monocytes in the peritoneal cavity (**Fig. S8D**) and a more intense expression of CD38 and PD-L1 was observed in cells in mice treated with PMEL-IL-12 compared with those transferred with PMEL-1-LUC.

In general, IL-12 electroporation endows exogenous PMEL-1 T cells and the studied endogenous immune cell populations with a similar, though less active phenotype when compared to that observed in the OT-I model.

To further potentiate the therapeutic efficacy of the approach, we combined the adoptive transfer with the immune checkpoint blocking antibody anti-PD-1 or an agonist antibody for the costimulatory molecule CD137. Both combinations potentiated the efficacy of the locoregional engineered T cell delivery strategy, significantly increasing overall survival with respect to the PMEL-1-IL-12 treatment alone (Figure 5d).

Discussion

Peritoneal carcinomatosis represents a metastatic stage from which patients often die within 2 to 6 months after the condition becomes apparent in imaging studies. To improve such a dismal prognosis, current research focuses on two major strategies: *i)* improving the early diagnosis of PCa,[53] and *ii)* discovering novel interventions with an advantageous therapeutic index. Within the peritoneal cavity, the omentum represents a favorable site for metastasis, which eventually becomes subjugated to the tumor and contributes to its growth. The omentum is a visceral peritoneal fold that consists of multiple sheets of mesothelial cells surrounding highly vascularized adipose tissue and lymphoid aggregates, historically defined as "milky spots". In this setting, immunotherapy is an attractive strategy, as it aims at awakening the immune system against malignancies.

We have tested the anti-tumor efficacy of tumor-specific T lymphocytes, *ex vivo* electroporated with a single-chain IL-12-coding mRNA,[29] into mice bearing tumors localized to the omentum. IL-12 is an extremely potent pro-inflammatory cytokine whose persistent expression-dependent toxicity is the main obstacle to its clinical application. In fact, intravenous administration of the recombinant protein was responsible for the death of two patients in 1997 in a phase II clinical trial.[54] IL-12 has previously been used as a cytokine to engineer adoptive transfer therapies, in mouse models and in the clinic.[25–28,29,55] In these settings, several strategies are being exploited to limit IL-12-dependent toxicities: *i)* the expression of the induced protein is set under the control of the NFAT minimal promoter, which is activated after antigen recognition,[25] *ii)* elimination genes are inserted into the CAR-cytokine construct (NCT02498912) or *iii)* the heterodimeric cytokine is tethered to the plasma membrane, by inserting it into the extracellular moiety of a CAR.[27] *iv)* We decided to employ the strategy that exploits the intrinsic transient nature of the mRNA molecule[56] and the potential of such an approach has been previously demonstrated by intra-tumoral administration in mice

bearing subcutaneous tumors. In this report, a potent anti-tumor effect was observed in the treated lesion and the activation of an endogenous cDC1-dependent immune response. This treatment scheme also achieved efficacy against distant non-injected lesions.[29] To continue this work, we have evaluated whether intracavitary delivery of these engineered T cells could be used for the treatment of peritoneal metastases. In a model of intraperitoneal disease, we compared IP *vs.* IV treatments, and our results demonstrate the marked superiority of the intraperitoneal route, confirming the findings of other laboratories.[20] Transferred T cells administered intraperitoneally homed to the omentum as soon as 5 h after their injection (Figure 1d). This preferential localization did not depend on the presence of tumor in the omentum and was significantly higher if compared to T cells reaching the spleen or other intraperitoneal organs such the mesentery (Figure 1d and **Fig. S1B, C**). Electroporated IL-12 was correctly expressed and detected in peritoneal lavage fluids and sera from tumor-free and tumor-bearing mice (Figure 1e, Figure 2a and **Figure S2A**). IL-12, by binding its heterodimeric receptors on activated T cells, NK and NKT cells, predominantly triggers Jak-STAT4-mediated intracellular signaling, leading to the transcription and secretion of IFN-γ,[57] which is considered one of the most potent downstream effectors of IL-12 in cancer treatment[58] and is known to further amplify IL-12 production.[59] We were expecting similar IFN-γ levels systemically, being the levels of IL-12 comparable for the two different routes of administration (**Fig. S2** and Figures 1e-f). Perhaps, at the time point studied, it was too early to observe such direct induction, but it was sufficient to observe the cascade triggered by the OT-I direct first-pass localization to the tumor site. Indeed, as shown by the comparison between the tumor-bearing and tumor-free mice treated with the locoregional or systemic route (Figure 2a and **Fig. S2A**), the rapid encounter of the T cells with the OVA antigen in the tumor-bearing omentum induced a cascade of pro-inflammatory cytokines, including IFN-γ, IL-6, IL-2 and TNF-α and chemoattractant proteins. Compared to the systemic route, locoregional treatment also induced a stronger up-regulation of the transcripts of T cell chemotactic proteins such as CXCL10, CXCL11, CXCL16, and CCL5 and the down-regulation of M2-polarized macrophages markers, such as CD209f[60] (Figure 3a and **Fig. S3**). Furthermore, IL-12 induced higher levels of markers of a Th1 immune response such TNF-α, granzyme B, IFN-γ, perforin1 and other pro-inflammatory cytokines such as IL-6, IL-1α, IL-1β, IL-2Rα, IL-33 and its receptor (Figure 3f, g and **Fig. S3**). This last cytokine has previously been shown to delay metastatic peritoneal cancer progression.[61,62] Among the down-regulated genes with respect to the intravenous route, the fatty acid metabolic category was strongly dampened (Figure 3d, e). Cancer cells up-regulate this pathway to support the aberrant growth and proliferation of cells. Under conditions of metabolic stress, cancer cells up-regulate ACSS2 which is necessary to generate acetyl-CoA, FABP4 that facilitates extracellular scavenging of long-chain unsaturated lysophospholipids that can be used as a nutrient source, and FASN involved in *de novo* lipogenesis.[63] These three genes were found down-regulated after intraperitoneal administration of IL-12-engineered T lymphocytes (Figure 3e).

It is noteworthy that electroporation of IL-12 mRNA contributes to overcoming the main hurdles to applying adoptive T cell therapy to solid tumors. First, it endows T cells with a

longer persistence in the omentum, spleen, peritoneal cavity, and peripheral blood of mice as compared to those electroporated with irrelevant mRNA (Figure 4a-e). The higher persistence of T cells in mice could be partially explained by some of the RNA-Seq results. In 2014, Starbeck-Miller et al. proposed two models to explain how signal 3 cytokines, such as IL-12, prolonged the survival of T cells.[64] The first is that type-3 signals inhibit the apoptosis cascade by upregulating Bcl3.[65,66] In fact, we observed an up-regulation of the Bcl3 transcript in OT-I-IL-12-treated mice, with a slight increase in locoregional over the systemic route (**Fig. S3B**).

The second model proposes that IL-12 prolongs survival by increasing the expression of IL-2Rα[67] and IL-2Rβ.[38] At the studied time point, up-regulation of IL-2Rα is observed both the bulk RNA-Seq of omentum (Figure 3 and **Fig. S3**) and in flow cytometry staining of transferred T cells isolated from the peritoneal cavity and omentum (**Fig. S4**), suggesting that the treatment provides a proliferative advantage to CD8^{+} T cells at early time points after injection.

Second, IL-12 engineering of the tumor-specific lymphocytes prevents tumor escape due to antigen loss, at least in the OT-I-B16-OVA setting. In fact, injection of IL-12-OT-I IP promoted the acquisition of immunity against endogenous B16 antigens, with >80% of mice being able to reject an SC rechallenge with the parental cell line (Figure 4f, g). IFN-γ is known to induce up-regulation of MHC-I,[68] thus fostering antigenic presentation of tumor antigens, leading to the acquisition of specific anti-tumor immunity against antigens different from those targeted by the therapy in the first place.

The third limitation that weakens the efficacy of ACT and that IL-12 is able to overcome is the immunosuppressive TME.[69] In fact, apart from the transcriptional reprogramming found through the bulk RNA-Seq (Figure 3, **Fig. S3**), we observed how the engineering of IL-12-mRNA, compared to LUC-mRNA, increased the proliferation and acquisition of an activation phenotype of exogenous and endogenous CD8^{+} T cells and NK cells in the peritoneal cavity and omentum (**Fig. S4, Fig. S5A, B**). Furthermore, the IL-12-IFN-γ axis is known to exert powerful effects on the myeloid compartment and, in the peritoneal cavity, this consists of two populations: the large peritoneal macrophages and the small peritoneal macrophages. The first is the most abundant subset under steady-state conditions, characterized by high levels of F4/80, low levels of MHC-II and Tim-4 expression, and it originates from embryogenic precursors. The second is a rarer F4/80[low] MHC-II[high] population of monocyte-derived cells. Notably, LPMs have been associated with the promotion of metastatic peritoneal spread in humanized murine models of ovarian cancer and their depletion has been shown to promote a significant decrease of tumor burden in the omentum and the progression of malignant ascites. This is because such depletion hinders cancer cells from acquiring a stem cell phenotype,[5] reduces neoangiogenesis[42] and prevents such cells from sequestering and altering the proliferation of CD8^{+} T cells, as demonstrated in a murine model of colon carcinoma.[43] Interestingly, the injection of tumor-specific OT-I T cells induced an almost total ablation of the LPM population less than 24 h after IP delivery (**Fig. S5C**). "Macrophage disappearance reaction" (MDR) is a well-known phenomenon and has been demonstrated in several models of sterile inflammation

in the peritoneum and the extent of this loss depends on the stimulus and the severity of inflammation.[70] We believe that, because of the extremely high affinity of the OT-I transgenic TCR, the antigen recognition and the following downstream signaling cascade are sufficient to promote such a strong depletion. This phenomenon is accompanied by a compensatory increase in inflammatory monocytes (**Fig. S5D**). We have not investigated how long the contraction of the LPM population persists, but given the inverse correlation of the presence of this population with PCa prognosis, we can speculate that the strong depletion, together with the activation of the lymphocyte populations, supports the creation of an early favorable environment that contributes to the consistent eradication of tumors.

The fourth limitation of adoptive T cell transfer-based approaches consists of the poor tumor penetration of therapeutic T cells and, in our approach, this is overcome by the delivery method itself. In fact, locoregional injection favors T cell homing to the tumor-bearing omentum contributing to more potent anti-tumor efficacy. The relevance of this finding has been confirmed by recapitulating the potent anti-tumor effect in pancreatic tumor-IP bearing mice (Figure 5a) and by employing intermediate affinity TCR-transgenic T lymphocytes. Indeed, electroporation of IL-12 mRNA empowers PMEL-1 T cells, with respect to irrelevant mRNA, in the fight against the highly aggressive melanoma tumor B16-F10 (Figure 5b). However, in this scenario, transient armored-adoptive transfer achieves lower levels of IL-12 in vivo, compared to OT-I T cells, even if the efficacy of secreting IL-12 and IFN-γ after electroporation is comparable in vitro among the two models (Figure 5c, **Fig. S6A, B**). We must consider that in vitro both cognate antigenic peptides (OVA$_{257-264}$ and human gp100$_{25-33}$) are used in saturating conditions, and this leads to a comparable expression of IL-12. However, we must also take in account that in vivo the murine gp100$_{25-33}$ is presented on MHC-I molecules 100 times less efficiently than the human antigenic peptide,[52] and that the affinity of PMEL-1 TCR is 1000 times lower compared to OT-I-TCR.[71,72] These facts may explain the lower induction of TCR engagement. The strength of the latter has been positively correlated with the activation of the translation machinery and ribosome biogenesis in lymphocytes.[73] This would explain the lower concentration of IL-12 attained in vivo and, consequently, the weaker pro-inflammatory reprogramming of the TME, the less active phenotype of the immune subsets under investigation, and the weaker contraction of the LPM population that we observed in PMEL-1 setting compared to the OT-I model (**Fig. S7, Fig S8**). However, there is room for improvement. In fact, by combining this IL-12-PMEL-1 adoptive transfer strategy with anti-PD-1 checkpoint blockade or with agonistic CD137 costimulatory signaling, the therapeutic efficacy is significantly increased (Figure 5d). More optimizations could be performed, including the administration of a higher number of doses, the electroporation of a more elevated concentration of the mRNA, and the injection of increased number of tumor-specific T lymphocytes. Another strategy that could significantly increase the therapeutic efficacy is the lymphodepletion prior to ACT to eliminate the competing cell populations and give transferred PMEL-1 cells a survival advantage. As already performed in clinical adoptive T cell therapy, this approach

could be further strengthened by multiple injections of recombinant IL-2 to foster the expansion and activation of adoptively transferred T cells.[74]

Overall, our strategy combines the advantages of proinflammatory cytokine-coding mRNA that mitigates the potential toxicities related to sustained expression, together with the locoregional intracavitary treatment to increase the exposure of tumor antigens to the transferred tumor-specific T lymphocytes armored with IL-12. RNA-engineering of T cells is already a reality in clinical trials[75,76] and intraperitoneal injection has been used for decades for the delivery of chemotherapeutic agents.[77] To the best of our knowledge, this route has been employed for adoptive T cell therapy in clinical peritoneal carcinomatosis only in two cases to date (NCT02498912, NCT03682744). Additionally, there are some local treatment experiences related to CAR T delivery such as in brain ventricles for glioblastoma[78] and in the pleural cavity for mesothelioma.[79] Our data point to an alternative and safer route for the intracavitary delivery of adoptive T cell therapies that deserves clinical testing, especially when considering the transient engineering with interleukin 12[80] and other proinflammatory transgenes.

Acknowledgments

Disclosure statement

I.M. reports advisory roles with Roche-Genentech, Bristol-Myers Squibb, CYTOMX, Incyte, MedImmune, Tusk, F-Star, Genmab, Molecular Partners, Alligator, Bioncotech, MSD, Merck Serono, Boehringer Ingelheim, Astra Zeneca, Numab, Catalym, and Bayer, and research funding from Roche, BMS, Alligator, and Highlight Therapeutics. MA reports receiving research funding from Highlight Therapeutics and PharmaMar. The rest of the authors have no conflict of interest to declare.

Funding

ORCID

Fernando Aranda http://orcid.org/0000-0002-9364-474X

References

1. Coccolini F, Gheza F, Lotti M, Virzì S, Iusco D, Ghermandi C, Melotti R, Baiocchi G, Giulini SM, Ansaloni L, et al. Peritoneal carcinomatosis. World J Gastroenterol. 2013;19(41):6979–6994. doi:10.3748/wjg.v19.i41.6979.
2. Terzi C. Peritoneal carcinomatosis of gastrointestinal tumors: where are we now? World J Gastroenterol. 2014;20(39):14371–14380. doi:10.3748/wjg.v20.i39.14371.
3. van Baal J, van Noorden Cjf, Nieuwland R, Van de Vijver KK, Sturk A, van Driel Wj, Kenter GG, Lok CAR, van Noorden CJF, van Driel WJ. Development of peritoneal carcinomatosis in epithelial ovarian cancer: a review. J Histochem Cytochem. 2018;66(2):67–83. doi:10.1369/0022155417742897.
4. Cortes-Guiral D, Hubner M, Alyami M, Bhatt A, Ceelen W, Glehen O, Lordick F, Ramsay R, Sgarbura O, Van Der Speeten K, et al. Primary and metastatic peritoneal surface malignancies. Nat Rev Dis Primers. 2021;7(1):91. doi:10.1038/s41572-021-00326-6
5. Etzerodt A, Moulin M, Doktor TK, Delfini M, Mossadegh-Keller N, Bajenoff M, Sieweke MH, Moestrup SK, Auphan-Anezin N, Lawrence T. Tissue-resident macrophages in omentum promote metastatic spread of ovarian cancer. J Exp Med. 2020;217(4). doi:10.1084/jem.20191869.
6. Lee W, Ko SY, Mohamed MS, Kenny HA, Lengyel E, Naora H. Neutrophils facilitate ovarian cancer premetastatic niche formation in the omentum. J Exp Med. 2019;216(1):176–194. doi:10.1084/jem.20181170.
7. Platell C, Cooper D, Papadimitriou JM, Hall JC. The omentum. World J Gastroenterol. 2000;6(2):169–176. doi:10.3748/wjg.v6.i2.169.
8. Koppe MJ, Nagtegaal ID, de Wilt Jh, Ceelen WP, de Wilt JHW. Recent insights into the pathophysiology of omental metastases. J Surg Oncol. 2014;110(6):670–675. doi:10.1002/jso.23681.
9. Nieman KM, Kenny HA, Penicka CV, Ladanyi A, Buell-Gutbrod R, Zillhardt MR, Romero IL, Carey MS, Mills GB, Hotamisligil GS, et al. Adipocytes promote ovarian cancer metastasis and provide energy for rapid tumor growth. Nat Med. 2011;17(11):1498–1503. doi:10.1038/nm.2492.
10. Gerber SA, Rybalko VY, Bigelow CE, Lugade AA, Foster TH, Frelinger JG, Lord EM. Preferential attachment of peritoneal tumor metastases to omental immune aggregates and possible role of a unique vascular microenvironment in metastatic survival and growth. Am J Pathol. 2006;169(5):1739–1752. doi:10.2353/ajpath.2006.051222.
11. Liu Y, Hu JN, Luo N, Zhao J, Liu SC, Ma T, Yao YM. The essential involvement of the omentum in the peritoneal defensive mechanisms during intra-abdominal sepsis. Front Immunol. 2021;12:631609. doi:10.3389/fimmu.2021.631609.
12. Beelen RH. Role of omental milky spots in the local immune response. Lancet. 1992;339(8794):689. doi:10.1016/0140-6736(92)90857-y.
13. Liu M, Silva-Sanchez A, Randall TD, Meza-Perez S. Specialized immune responses in the peritoneal cavity and omentum. J Leukoc Biol. 2021;109(4):717–729. doi:10.1002/JLB.5MIR0720-271RR.
14. Meza-Perez S, Randall TD. Immunological Functions of the Omentum. Trends Immunol. 2017;38(7):526–536. doi:10.1016/j.it.2017.03.002.
15. Bella A, Arrizabalaga L, Di Trani CA, Fernandez-Sendin M, Teijeira A, Russo-Cabrera JS, Melero I, Berraondo P, Aranda F. Omentum: friend or foe in ovarian cancer immunotherapy? Int Rev Cell Mol Biol. 2022;371:117–131. doi:10.1016/bs.ircmb.2022.04.017.
16. Chia CS, You B, Decullier E, Vaudoyer D, Lorimier G, Abboud K, Bereder JM, Arvieux C, Boschetti G, Glehen O, et al. Patients with peritoneal carcinomatosis from gastric cancer treated with cytoreductive surgery and hyperthermic intraperitoneal chemotherapy: is cure a possibility? Ann Surg Oncol. 2016;23(6):1971–1979. doi:10.1245/s10434-015-5081-3.
17. Gamboa AC, Winer JH. Cytoreductive surgery and hyperthermic intraperitoneal chemotherapy for gastric cancer. Cancers (Basel). 2019;11(11):1662. doi:10.3390/cancers11111662.

18. Malfroy S, Wallet F, Maucort-Boulch D, Chardonnal L, Sens N, Friggeri A, Passot G, Glehen O, Piriou V. Complications after cytoreductive surgery with hyperthermic intraperitoneal chemotherapy for treatment of peritoneal carcinomatosis: risk factors for ICU admission and morbidity prognostic score. Surg Oncol. 2016;25(1):6–15. doi:10.1016/j.suronc.2015.11.003.

19. Lenzi R, Edwards R, June C, Seiden MV, Garcia ME, Rosenblum M, Freedman RS. Phase II study of intraperitoneal recombinant interleukin-12 (rhIL-12) in patients with peritoneal carcinomatosis (residual disease < 1 cm) associated with ovarian cancer or primary peritoneal carcinoma. J Transl Med. 2007;5:66. doi:10.1186/1479-5876-5-66.

20. Katz SC, Point GR, Cunetta M, Thorn M, Guha P, Espat NJ, Boutros C, Hanna N, Junghans RP. Regional CAR-T cell infusions for peritoneal carcinomatosis are superior to systemic delivery. Cancer Gene Ther. 2016;23(5):142–148. doi:10.1038/cgt.2016.14.

21. Orr B, Mahdi H, Fang Y, Strange M, Uygun I, Rana M, Zhang L, Suarez Mora A, Pusateri A, Elishaev E, et al. Phase I trial combining chemokine-targeting with loco-regional chemoimmunotherapy for recurrent, platinum-sensitive ovarian cancer shows induction of CXCR3 ligands and markers of type 1 immunity. Clin Cancer Res. 2022;28(10):2038–2049. doi:10.1158/1078-0432.CCR-21-3659.

22. Thadi A, Khalili M, Morano WF, Richard SD, Katz SC, Bowne WB. Early investigations and recent advances in intraperitoneal immunotherapy for peritoneal metastasis. Vaccines (Basel). 2018;6(3). doi:10.3390/vaccines6030054.

23. Bella Á, Arrizabalaga L, Di Trani CA, Cirella A, Fernandez-Sendin M, Gomar C, Russo-Cabrera JS, Rodriguez I, Gonzalez-Gomariz J, Alvarez M, et al. Synergistic antitumor response with recombinant modified virus Ankara armed with CD40L and CD137L against peritoneal carcinomatosis. Oncoimmunology. 2022;11(1):2098657. doi:10.1080/2162402X.2022.2098657.

24. Sterner RC, Sterner RM. CAR-T cell therapy: current limitations and potential strategies. Blood Cancer J. 2021;11(4):69. doi:10.1038/s41408-021-00459-7.

25. Chmielewski M, Kopecky C, Hombach AA, Abken H. IL-12 release by engineered T cells expressing chimeric antigen receptors can effectively Muster an antigen-independent macrophage response on tumor cells that have shut down tumor antigen expression. Cancer Res. 2011;71(17):5697–5706. doi:10.1158/0008-5472.CAN-11-0103.

26. Koneru M, Purdon TJ, Spriggs D, Koneru S, Brentjens RJ. IL-12 secreting tumor-targeted chimeric antigen receptor T cells eradicate ovarian tumors in vivo. Oncoimmunology. 2015;4(3):e994446. doi:10.4161/2162402X.2014.994446.

27. Hombach A, Barden M, Hannappel L, Chmielewski M, Rappl G, Sachinidis A, Abken H. IL12 integrated into the CAR exodomain converts CD8+ T cells to poly-functional NK-like cells with superior killing of antigen-loss tumors. Mol Ther. 2022;30(2):593–605. doi:10.1016/j.ymthe.2021.10.011.

28. Koneru M, O'Cearbhaill R, Pendharkar S, Spriggs DR, Brentjens RJ. A phase I clinical trial of adoptive T cell therapy using IL-12 secreting MUC-16ecto directed chimeric antigen receptors for recurrent ovarian cancer. J Transl Med. 2015;13(1):102. doi:10.1186/s12967-015-0460-x.

29. Etxeberria I, Bolanos E, Quetglas JI, Gros A, Villanueva A, Palomero J, Sanchez-Paulete AR, Piulats JM, Matias-Guiu X, Olivera I, et al. Intratumor Adoptive Transfer of IL-12 mRNA transiently engineered antitumor CD8(+) T Cells. Cancer Cell. 2019;36(6):613–629 e7. doi:10.1016/j.ccell.2019.10.006.

30. Bella Á, Di Trani CA, Fernández-Sendin M, Arrizabalaga L, Cirella A, Teijeira Á, Medina-Echeverz J, Melero I, Berraondo P, Aranda F. Mouse Models of Peritoneal Carcinomatosis to Develop Clinical Applications. Cancers. 2021;13(5):963. doi:10.3390/cancers13050963.

31. Lieschke GJ, Rao PK, Gately MK, Mulligan RC. Bioactive murine and human interleukin-12 fusion proteins which retain antitumor activity in vivo. Nat Biotechnol. 1997;15(1):35–40. doi:10.1038/nbt0197-35.

32. Holtkamp S, Kreiter S, Selmi A, Simon P, Koslowski M, Huber C, Tureci O, Sahin U. Modification of antigen-encoding RNA increases stability, translational efficacy, and T-cell stimulatory

33. capacity of dendritic cells. Blood. 2006;108(13):4009–4017. doi:10.1182/blood-2006-04-015024.

33. Bolger AM, Lohse M, Usadel B. Trimmomatic: a flexible trimmer for Illumina sequence data. Bioinformatics. 2014;30(15):2114–2120. doi:10.1093/bioinformatics/btu170.

34. Dobin A, Davis CA, Schlesinger F, Drenkow J, Zaleski C, Jha S, Batut P, Chaisson M, Gingeras TR. STAR: ultrafast universal RNA-seq aligner. Bioinformatics. 2013;29(1):15–21. doi:10.1093/bioinformatics/bts635.

35. Ritchie ME, Phipson B, Wu D, Hu Y, Law CW, Shi W, Smyth GK. limma powers differential expression analyses for RNA-sequencing and microarray studies. Nucleic Acids Research. 2015;43(7):e47–e47. doi:10.1093/nar/gkv007.

36. Wu T, Hu E, Xu S, Chen M, Guo P, Dai Z, Feng T, Zhou L, Tang W, Zhan L, et al. clusterProfiler 4.0: a universal enrichment tool for interpreting omics data. Innovation (N Y). 2021;2(3):100141. doi:10.1016/j.xinn.2021.100141.

37. Weiss JM, Davies LC, Karwan M, Ileva L, Ozaki MK, Cheng RY, Ridnour LA, Annunziata CM, Wink DA, McVicar DW. Itaconic acid mediates crosstalk between macrophage metabolism and peritoneal tumors. J Clin Invest. 2018;128(9):3794–3805. doi:10.1172/JCI99169.

38. Valenzuela J, Schmidt C, Mescher M. The roles of IL-12 in providing a third signal for clonal expansion of naive CD8 T cells. J Immunol. 2002;169(12):6842–6849. doi:10.4049/jimmunol.169.12.6842.

39. Zhao Y, Ohdan H, Manilay JO, Sykes M. NK cell tolerance in mixed allogeneic chimeras. J Immunol. 2003;170(11):5398–5405. doi:10.4049/jimmunol.170.11.5398.

40. Zhang L, Kerkar SP, Yu Z, Zheng Z, Yang S, Restifo NP, Rosenberg SA, Morgan RA. Improving adoptive T cell therapy by targeting and controlling IL-12 expression to the tumor environment. Mol Ther. 2011;19(4):751–759. doi:10.1038/mt.2010.313.

41. Kerkar SP, Goldszmid RS, Muranski P, Chinnasamy D, Yu Z, Reger RN, Leonardi AJ, Morgan RA, Wang E, Marincola FM, et al. IL-12 triggers a programmatic change in dysfunctional myeloid-derived cells within mouse tumors. J Clin Invest. 2011;121(12):4746–4757. doi:10.1172/JCI58814.

42. Robinson-Smith TM, Isaacsohn I, Mercer CA, Zhou M, Van Rooijen N, Husseinzadeh N, McFarland-Mancini MM, Drew AF. Macrophages mediate inflammation-enhanced metastasis of ovarian tumors in mice. Cancer Res. 2007;67(12):5708–5716. doi:10.1158/0008-5472.CAN-06-4375.

43. Chow A, Schad S, Green MD, Hellmann MD, Allaj V, Ceglia N, Zago G, Shah NS, Sharma SK, Mattar M, et al. Tim-4+ cavity-resident macrophages impair anti-tumor CD8+ T cell immunity. Cancer Cell. 2021;39(7):973–988 e9. doi:10.1016/j.ccell.2021.05.006.

44. Liu Z, Gu Y, Chakarov S, Bleriot C, Kwok I, Chen X, Shin A, Huang W, Dress RJ, Dutertre C-A, et al. Fate mapping via ms4a3-expression history traces monocyte-derived cells. Cell. 2019;178(6):1509–1525 e19. doi:10.1016/j.cell.2019.08.009.

45. Bauvois B, Durant L, Laboureau J, Barthelemy E, Rouillard D, Boulla G, Deterre P. Upregulation of CD38 gene expression in leukemic B cells by interferon types I and II. J Interferon Cytokine Res. 1999;19(9):1059–1066. doi:10.1089/107999099313299.

46. Amici SA, Young NA, Narvaez-Miranda J, Jablonski KA, Arcos J, Rosas L, Papenfuss TL, Torrelles JB, Jarjour WN, Guerau-de-Arellano M. CD38 is robustly induced in human macrophages and monocytes in inflammatory conditions. Front Immunol. 2018;9:1593. doi:10.3389/fimmu.2018.01593.

47. Deaglio S, Morra M, Mallone R, Ausiello CM, Prager E, Garbarino G, Dianzani U, Stockinger H, Malavasi F. Human CD38 (ADP-ribosyl cyclase) is a counter-receptor of CD31, an Ig superfamily member. J Immunol. 1998;160:395–402.

48. Kang J, Park KH, Kim JJ, Jo EK, Han MK, Kim UH. The role of CD38 in Fcgamma receptor (FcgammaR)-mediated phagocytosis in murine macrophages. J Biol Chem. 2012;287(18):14502–14514. doi:10.1074/jbc.M111.329003.

49. Zilber MT, Setterblad N, Vasselon T, Doliger C, Charron D, Mooney N, Gelin C. MHC class II/CD38/CD9: a lipid-raft-dependent signaling complex in human monocytes. Blood. 2005;106(9):3074–3081. doi:10.1182/blood-2004-10-4094.

50. Thomassen I, Lemmens VE, Nienhuijs SW, Luyer MD, Klaver YL, de Hingh IH. Incidence, prognosis, and possible treatment strategies of peritoneal carcinomatosis of pancreatic origin: a population-based study. Pancreas. 2013;42(1):72–75. doi:10.1097/MPA.0b013e31825abf8c.

51. Overwijk WW, Theoret MR, Finkelstein SE, Surman DR, de Jong LA, Vyth-Dreese FA, Dellemijn TA, Antony PA, Spiess PJ, Palmer DC, et al. Tumor regression and autoimmunity after reversal of a functionally tolerant state of self-reactive CD8+ T cells. J Exp Med. 2003;198(4):569–580. doi:10.1084/jem.20030590.

52. Overwijk WW, Tsung A, Irvine KR, Parkhurst MR, Goletz TJ, Tsung K, Carroll MW, Liu C, Moss B, Rosenberg SA, et al. gp100/pmel 17 is a murine tumor rejection antigen: induction of "self"-reactive, tumoricidal T cells using high-affinity, altered peptide ligand. J Exp Med. 1998;188(2):277–286. doi:10.1084/jem.188.2.277.

53. McMullen JRW, Selleck M, Wall NR, Senthil M. Peritoneal carcinomatosis: limits of diagnosis and the case for liquid biopsy. Oncotarget. 2017;8(26):43481–43490. doi:10.18632/oncotarget.16480.

54. Leonard JP, Sherman ML, Fisher GL, Buchanan LJ, Larsen G, Atkins MB, Sosman JA, Dutcher JP, Vogelzang NJ, Ryan JL. Effects of single-dose interleukin-12 exposure on interleukin-12-associated toxicity and interferon-gamma production. Blood. 1997;90:2541–2548.

55. Di Trani CA, Cirella A, Arrizabalaga L, Fernandez-Sendin M, Bella A, Aranda F, Melero I, Berraondo P. Overcoming the limitations of cytokines to improve cancer therapy. Int Rev Cell Mol Biol. 2022;369:107–141. doi:10.1016/bs.ircmb.2022.05.002.

56. Gomez-Aguado I, Rodriguez-Castejon J, Beraza-Millor M, Rodriguez-Gascon A, Del Pozo-Rodriguez A, Solinis MA. mRNA delivery technologies: toward clinical translation. Int Rev Cell Mol Biol. 2022;372:207–293. doi:10.1016/bs.ircmb.2022.04.010.

57. Morinobu A, Gadina M, Strober W, Visconti R, Fornace A, Montagna C, Feldman GM, Nishikomori R, O'Shea JJ. STAT4 serine phosphorylation is critical for IL-12-induced IFN-gamma production but not for cell proliferation. Proc Natl Acad Sci U S A. 2002;99(19):12281–12286. doi:10.1073/pnas.182618999.

58. Berraondo P, Sanmamed MF, Ochoa MC, Etxeberria I, Aznar MA, Perez-Gracia JL, Rodriguez-Ruiz ME, Ponz-Sarvise M, Castanon E, Melero I. Cytokines in clinical cancer immunotherapy. Br J Cancer. 2019;120(1):6–15. doi:10.1038/s41416-018-0328-y.

59. Tugues S, Burkhard SH, Ohs I, Vrohlings M, Nussbaum K, Vom Berg J, Kulig P, Becher B. New insights into IL-12-mediated tumor suppression. Cell Death Differ. 2015;22(2):237–246. doi:10.1038/cdd.2014.134.

60. Cao X, Lai SWT, Chen S, Wang S, Feng M. Targeting tumor-associated macrophages for cancer immunotherapy. Int Rev Cell Mol Biol. 2022;368:61–108. doi:10.1016/bs.ircmb.2022.02.002.

61. Perales-Puchalt A, Svoronos N, Villarreal DO, Zankharia U, Reuschel E, Wojtak K, Payne KK, Duperret EK, Muthumani K, Conejo-Garcia JR, et al. IL-33 delays metastatic peritoneal cancer progression inducing an allergic microenvironment. Oncoimmunology. 2019;8(1):e1515058. doi:10.1080/2162402X.2018.1515058.

62. Villarreal DO, Wise MC, Walters JN, Reuschel EL, Choi MJ, Obeng-Adjei N, Yan J, Morrow MP, Weiner DB. Alarmin IL-33 acts as an immunoadjuvant to enhance antigen-specific tumor immunity. Cancer Res. 2014;74(6):1789–1800. doi:10.1158/0008-5472.CAN-13-2729.

63. Koundouros N, Poulogiannis G. Reprogramming of fatty acid metabolism in cancer. Br J Cancer. 2020;122(1):4–22. doi:10.1038/s41416-019-0650-z.

64. Starbeck-Miller GR, Xue HH, Harty JT. IL-12 and type I interferon prolong the division of activated CD8 T cells by maintaining high-affinity IL-2 signaling in vivo. J Exp Med. 2014;211(1):105–120. doi:10.1084/jem.20130901.

65. Mitchell TC, Hildeman D, Kedl RM, Teague TK, Schaefer BC, White J, Zhu Y, Kappler J, Marrack P. Immunological adjuvants promote activated T cell survival via induction of Bcl-3. Nat Immunol. 2001;2(5):397–402. doi:10.1038/87692.

66. Valenzuela JO, Hammerbeck CD, Mescher MF. Cutting edge: bcl-3 up-regulation by signal 3 cytokine (IL-12) prolongs survival of antigen-activated CD8 T cells. J Immunol. 2005;174(2):600–604. doi:10.4049/jimmunol.174.2.600.

67. Pipkin ME, Sacks JA, Cruz-Guilloty F, Lichtenheld MG, Bevan MJ, Rao A. Interleukin-2 and inflammation induce distinct transcriptional programs that promote the differentiation of effector cytolytic T cells. Immunity. 2010;32(1):79–90. doi:10.1016/j.immuni.2009.11.012.

68. Rosa FM, Fellous M. Regulation of HLA-DR gene by IFN-gamma. Transcriptional and post-transcriptional control. J Immunol. 1988;140:1660–1664.

69. Martin-Otal C, Navarro F, Casares N, Lasarte-Cia A, Sanchez-Moreno I, Hervas-Stubbs S, Lozano T, Lasarte JJ. Impact of tumor microenvironment on adoptive T cell transfer activity. Int Rev Cell Mol Biol. 2022;370:1–31. doi:10.1016/bs.ircmb.2022.03.002.

70. Louwe PA, Badiola Gomez L, Webster H, Perona-Wright G, Bain CC, Forbes SJ, Jenkins SJ. Recruited macrophages that colonize the post-inflammatory peritoneal niche convert into functionally divergent resident cells. Nat Commun. 2021;12(1):1770. doi:10.1038/s41467-021-21778-0.

71. Alam SM, Travers PJ, Wung JL, Nasholds W, Redpath S, Jameson SC, Gascoigne NR. T-cell-receptor affinity and thymocyte positive selection. Nature. 1996;381(6583):616–620. doi:10.1038/381616a0.

72. Uchtenhagen H, Abualrous ET, Stahl E, Allerbring EB, Sluijter M, Zacharias M, Sandalova T, van Hall T, Springer S, Nygren PA, et al. Proline substitution independently enhances H-2D(b) complex stabilization and TCR recognition of melanoma-associated peptides. Eur J Immunol. 2013;43(11):3051–3060. doi:10.1002/eji.201343456.

73. Tan TCJ, Knight J, Sbarrato T, Dudek K, Willis AE, Zamoyska R. Suboptimal T-cell receptor signaling compromises protein translation, ribosome biogenesis, and proliferation of mouse CD8 T cells. Proc Natl Acad Sci U S A. 2017;114(30):E6117–E6126. doi:10.1073/pnas.1700939114.

74. Rosenberg SA. IL-2: the first effective immunotherapy for human cancer. J Immunol. 2014;192(12):5451–5458. doi:10.4049/jimmunol.1490019.

75. Di Trani CA, Fernandez-Sendin M, Cirella A, Segues A, Olivera I, Bolanos E, Melero I, Berraondo P. Advances in mRNA-based drug discovery in cancer immunotherapy. Expert Opin Drug Discov. 2022;17(1):41–53. doi:10.1080/17460441.2021.1978972.

76. Pohl-Guimaraes F, Hoang-Minh LB, Mitchell DA. RNA-electroporated T cells for cancer immunotherapy. Oncoimmunology. 2020;9(1):1792625. doi:10.1080/2162402X.2020.1792625.

77. Markman M. Intraperitoneal antineoplastic drug delivery: rationale and results. Lancet Oncol. 2003;4(5):277–283. doi:10.1016/s1470-2045(03)01074-x.

78. Brown CE, Alizadeh D, Starr R, Weng L, Wagner JR, Naranjo A, Ostberg JR, Blanchard MS, Kilpatrick J, Simpson J, et al. Regression of glioblastoma after chimeric antigen receptor T-Cell Therapy. N Engl J Med. 2016;375(26):2561–2569. doi:10.1056/NEJMoa1610497.

79. Adusumilli PS, Zauderer MG, Riviere I, Solomon SB, Rusch VW, O'Cearbhaill RE, Zhu A, Cheema W, Chintala NK, Halton E, et al. A phase I trial of regional mesothelin-targeted CAR T-cell therapy in patients with malignant pleural disease, in combination with the Anti-PD-1 Agent Pembrolizumab. Cancer Discov. 2021;11(11):2748–2763. doi:10.1158/2159-8290.CD-21-0407.

80. Cirella A, et al. Novel strategies exploiting interleukin-12 in cancer immunotherapy. Pharmacol Ther. 2022: 108189.